Dalton Transactions

ROYAL SOCIETY OF CHEMISTRY

PAPER

View Article Online
View Journal | View Issue

Cite this: *Dalton Trans.*, 2024, **53**, 10737

Molecular engineering of 3-arylated tetrazo[1,2-*b*]indazoles: divergent synthesis and structure–property relationships†

Asmae Bousfiha,‡[a] Oumaima Abidi,‡[a] Louis Lemetayer,[b] Navya Sood,[a] Iogann Tolbatov,[a] Fabien Barrois,[a] Ahmad Daher,[a] Hélène Cattey,[a] Marie Cordier,[b] Muriel Hissler,[b] Jean-Cyrille Hierso,[a] Paul Fleurat-Lessard,*[a] Pierre-Antoine Bouit*[b] and Julien Roger*[a]

Received 16th April 2024,
Accepted 30th May 2024

DOI: 10.1039/d4dt01122h

rsc.li/dalton

The synthetic scope of 3-arylated tetrazo[1,2-*b*]indazoles is reported based on a Pd-catalyzed Liebeskind–Srogl cross-coupling reaction followed by an N-cyclisation process. The reactivity of the nitrogen atoms was used to further diversify these N-rich polyaromatic tetrazo[1,2-*b*]indazoles in a panel of reactions (protonation, selective oxidation, metallations). Selective *ortho*-C–H activation/functionalization on the heterocycle was also demonstrated with three transition metals (TM = Pd, Ir and Rh). The effects of all these molecular engineering strategies, particularly the N-modifications, on the optical and redox properties of the 3-arylated tetrazoindazoles were studied experimentally and theoretically. This study highlights the diversity of molecular structures and electronic properties offered by the tetrazo[1,2-*b*]indazole platform.

Introduction

Heterocycles containing nitrogen atoms are key building blocks for various applications ranging from biomedicine and agrochemistry to functional materials (explosives, optoelectronics). In the case of the latter application, aza-aromatics have shown great potential. Indeed, the presence of nitrogen atoms makes those compounds more electron-deficient than their all carbon-based counterparts and gives them excellent electron affinity. In addition, the specific reactivity of the nitrogen atom can be utilised to fine-tune their optical/redox properties at the molecular level, as well as those of the corresponding molecular materials.[1] Nitrogen-containing heteroaromatics, including among many others pyrazino[2,3-*b*:5,6-*b*′]diindolizines (**A**, Scheme 1) and azapyridazines (**B**, Scheme 1) have been developed for applications in optoelectronics or bioimaging.[2] However, in this field, the development of efficient synthetic approaches for innovative building blocks remains highly desirable, notably for safety and more atom-economy reasons. In this context, we have recently developed an unpre-

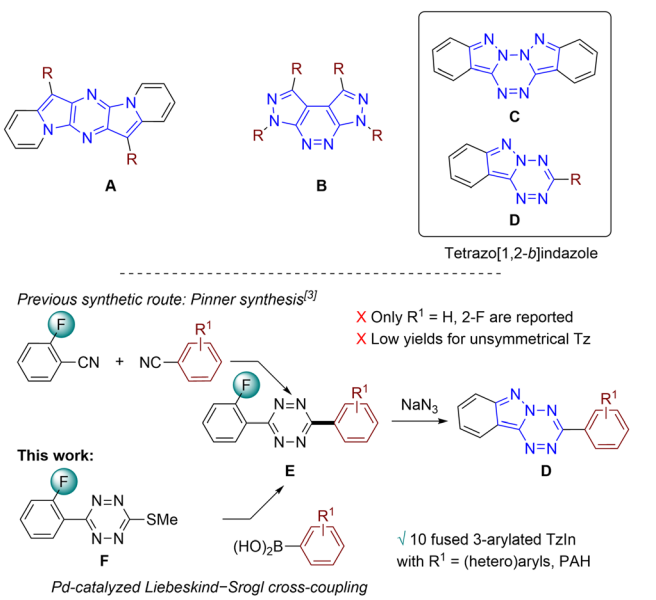

Scheme 1 N-rich heteroaromatics (top) and strategic routes to dissymmetric 3-aryltetrazo[1,2-*b*]indazoles (bottom, this work).

[a]*Institut de Chimie Moléculaire de l'Université de Bourgogne, UMR 6302 – Université Bourgogne (UB), 9, Avenue Alain Savary, 21078 Dijon, France.*
E-mail: julien.roger@u-bourgogne.fr, Paul.Fleurat-Lessard@u-bourgogne.fr
[b]*CNRS, ISCR – UMR 6226, Univ. Rennes, 35000 Rennes, France.*
E-mail: pierre-antoine.bouit@univ-rennes1.fr

†Electronic supplementary information (ESI) available: Experimental details and analytical data, NMR data and X-ray crystallographic data. CCDC 2307023 (**17-O1**), 2307024 (**17-O2**), 2332725 (**Rh**), 2332726 (**Pd**) and 2332727 (**Ir**). For ESI and crystallographic data in CIF or other electronic format see DOI: **https://doi.org/10.1039/d4dt01122h**

‡A. B. and O. A. contributed equally to this work.

cedented synthesis of tetrazo[1,2-*b*]indazoles (TzIn, **C** and **D**, Scheme 1) through the N–N cyclization of azido-functionalized *s*-tetrazines (Scheme 1, bottom).[3,4] These compounds exhibit a wide range of physico-chemical properties, depending on their molecular structure: low reduction potential, UV-vis absorption up to the near-infrared and intense fluorescence. However, this procedure gave limited access to structurally diverse tetrazo[1,2-*b*]indazoles **D**. This was due to the use of Pinner type synthesis to obtain the key fluoro-functionalized tetrazines (Tz) **E** (Scheme 1). Indeed, Pinner-type synthesis gives limited yields of *ortho*-functionalized products because of steric hindrance and side-reactivities especially when fluorine atoms are needed in *ortho*-position.[5] Moreover, the synthesis of unsymmetrical Tz in the presence of two different benzonitrile derivatives also furnished their corresponding symmetrical *s*-tetrazines. To overcome this issue, we envisaged a two steps strategy from 3-thiomethyltetrazines **F** (Scheme 1) as the key intermediate. This strategy allows for the divergent synthesis of arylated tetrazo[1,2-*b*]indazoles by employing a Pd-catalyzed Liebeskind–Srogl cross-coupling followed by a well-controlled N-cyclisation process.

We report the synthesis and characterization of a library of 3-arylated tetrazoindazoles. We explore the N-reactivity in various reactions (protonation, oxidation, coordination with transition metals). Furthermore, we demonstrate the selective *ortho*-C–H activation/functionalization on the TzIn scaffold using these TMs (Pd, Ir and Rh). Finally, we investigated the impact of these molecular engineering strategies on the optical and redox properties of these TzIn both experimentally and theoretically using density functional theory (DFT).

Results and discussion

Synthetic route to 3-aryltetrazo[1,2-*b*]indazoles

The recently disclosed heteroaromatic N-rich tetrazo[1,2-*b*] indazole is accessible from *ortho*-fluorinated aryl-*s*-tetrazine by a cascade azidation and intramolecular cyclisation process (Scheme 1, bottom).[3] Herein, we developed the access to diverse 3-arylated TzIn by a new synthetic route taking advantage of the divergent method reported by Fox *et al.* for the synthesis of unsymmetrical Tz.[6] In this approach, the key step is the Pd-catalyzed Liebeskind–Srogl cross-coupling on the 3-(thiomethyl)-6-(2-fluorophenyl)-tetrazine **F** (Scheme 1). In this key synthon **F**, the fluorine function, used for nucleophilic azidation substitution is introduced in the early steps of the synthesis. The pallado-catalyzed Liebeskind–Srogl cross-coupling reaction allowed the introduction of different aryls (Scheme 2).[7] The reaction afforded moderate to high isolated yields of 61–95% for **1–4** with *para* substituents (H, OMe, *t*Bu and NPh_2), while the *meta*-OMe **5** gave a 55% isolated yield. The symmetrical bis-3,6-(2-fluorophenyl)tetrazine **6** was obtained in the low isolated yield of 17% compared to our previous synthetic route, confirming that such a strategy is only versatile for preparing unsymmetrical building blocks.[5] As previously observed by Fox and coworkers,[6,7e] the bulky polyaromatic hydrocarbons and heteroarenes were found more challenging with lower conversions (Scheme 2). The 1-naphthyl and 9-phenanthryl were coupled in 32% and 53% yields for **7** and **8**, respectively. Finally, the 2-pyridenyl, 3-thienyl and 2-thienyl provided **9–11** in 22%, 50% and 23% isolated yields, respectively.

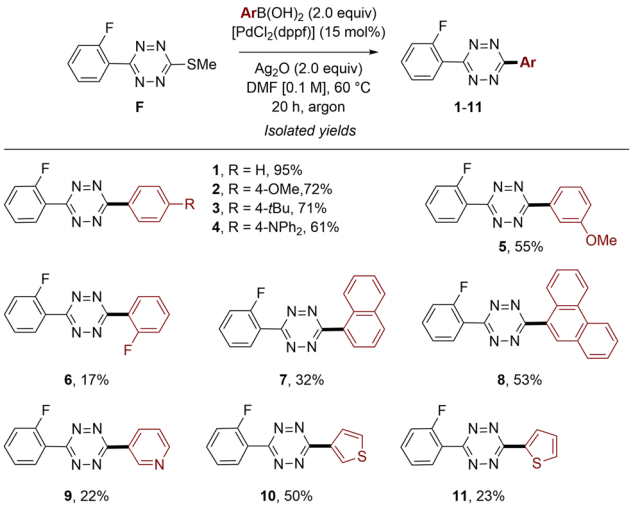

Scheme 2 Palladium-catalyzed Liebeskind–Srogl cross-coupling reaction for the synthesis of 3-aryl-6-(2-fluorophenyl)tetrazines.

The 3-arylated tetrazo[1,2-*b*]indazoles **12–22** were synthesized in the presence of 3 equivalents of NaN_3 in DMF using microwave irradiation (μW) for one hour at 130 °C (Scheme 3), following our previously reported procedure.[3] Under these conditions, the 3-phenyl-tetrazo[1,2-*b*]indazole **12** was isolated in 44% yield. The presence of donating substituents in the *para* (OMe, *t*Bu and NPh_2) or *meta* positions (OMe) improved the cyclization process slightly with 52%, 64%, 55% and 47% isolated yields for **13–16**, respectively. To favor the

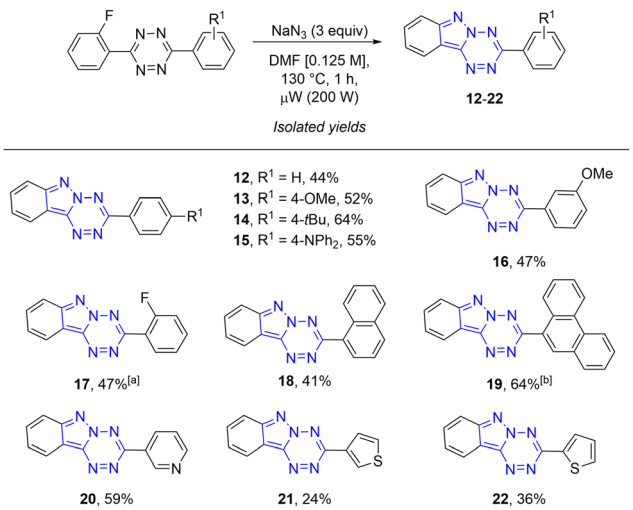

Scheme 3 Synthesis of the corresponding 3-aryl-tetrazo[1,2-*b*]indazoles. [a] 1 equiv. NaN_3; [b] 1.1 equiv. NaN_3 at 110 °C.

formation of the monocyclic 3-(2-fluorophenyl)-tetrazo[1,2-*b*] indazole **17** and limit the formation of the bis-tetrazo[1,2-*b*] indazoles,[5] the amount of sodium azide was reduced to only 1 equivalent to allow the formation of **17** in 47% isolated yield. The polyaromatic-substituted tetrazo[1,2-*b*]indazoles **18** and **19** were obtained in 41% and 64% isolated yields, respectively, after modifying the cyclization protocol for the 9-phenanthryl derivative (1.1 equivalents of NaN_3 at 110 °C). The 3-heteroarylated tetrazo[1,2-*b*]indazoles **20–22** were isolated in 59%, 24% and 36% isolated yields, respectively, principally due to a lack of reactivity and solubility.

This synthetic methodology, which combines a Pd-catalyzed Liebeskind–Srogl cross-coupling with an N_3-induced cyclization process, has significantly expanded the library of tetrazo [1,2-*b*]indazoles that was limited to poorly functionalized systems.[3]

Reactivity of the nitrogen core

The 3-(2-fluorophenyl)-tetrazo[1,2-*b*]indazole (**17**) was selected as a model to study the reactivity of these substrates (Schemes 4–7). First the reaction with acid was tested. Protonation of **17** using an excess of trifluoroacetic acid in $CDCl_3$ was evidenced by ^1H and ^{19}F NMR (see the ESI, Fig. S-3 and S-4†), illustrating that **17** is indeed prone to protonation. According to our DFT computation (see the ESI, Table S-Th1†), **17** should be protonated only on nitrogen N^1 (see Scheme 4 for numbering). Then N-oxide formation was tested, as such reactivity is characteristic of aromatic amino-heterocycles.[8] In the presence of an excess of trifluoroacetic anhydride and H_2O_2, the oxidation of **17** led to the formation of two products in a 50/50 ratio. X-ray diffraction allowed those products to be assigned to the derivatives where the N-oxidation had occurred selectively at N1 (**17-O1**) and N2 (**17-O2**) with 35% and 32% isolated yields (Scheme 4).

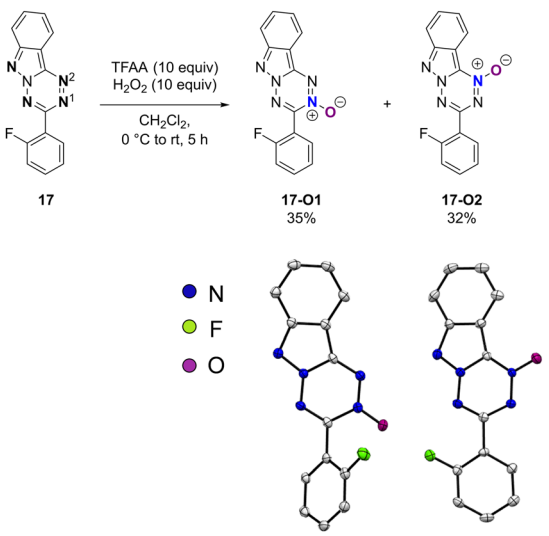

Scheme 4 N-oxide formation from **17**. Molecular structures of **17-O1** (left) and **17-O2** (right) (thermal ellipsoids at 30% probability, H atoms and CH_2Cl_2 are omitted for clarity).

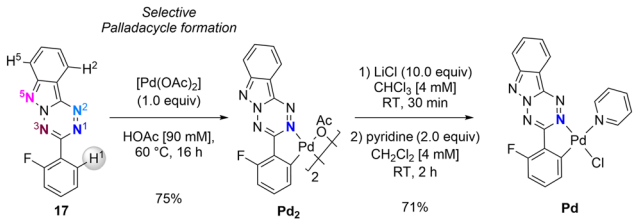

Scheme 5 Palladacycle synthesis with the 3-(2-fluorophenyl)-tetrazo [1,2-*b*]indazole (**17**). Only one isomer for **Pd** is represented for clarity.

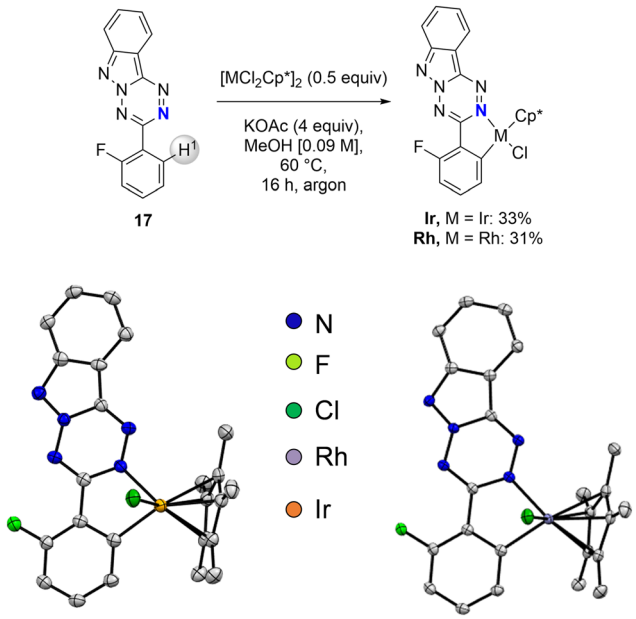

Scheme 6 Iridacycle and rhodacycle synthesis with the 3-(2-fluorophenyl)-tetrazo[1,2-*b*]indazole (**17**). Molecular structures of **Ir** (left) and **Rh** (right) (thermal ellipsoids at 30% probability, H atoms and CH_2Cl_2 are omitted for clarity).

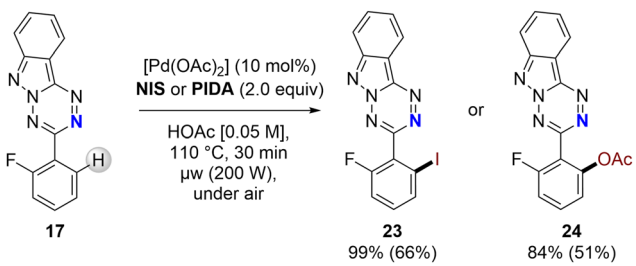

Scheme 7 N-directed palladium-catalyzed C–H bond functionalization of **17**. Conversion based on the consumption of **17** determined by ^1H and ^{19}F NMR ($CDCl_3$, 500 MHz and 470 MHz respectively), isolated yields in brackets.

Selective synthesis of metallacycles (M = Pd, Ir and Rh) from 17

We previously demonstrated that the use of the *N*-tetrazoindazole core as a directing group allows for N-directed palladium-catalyzed halogenation/acetoxylation

reactions.[3] Here we unambiguously show that the functionalization occurs with full selectivity on the *ortho*-position despite the presence of four different nitrogen atoms (Scheme 5, in color) which could potentially direct the C–H bond activation at three different *ortho*-positions (Scheme 5, H^1, H^2 or H^5). To clarify the origin of this selectivity trend, the formation of the metallacycle was studied computationally and experimentally.[9,10]

The dimeric palladacycle **Pd_2** was isolated in 75% yield by precipitation after reaction of $[Pd(OAc)_2]$ in HOAc (Scheme 5). Our attempts to crystallize the corresponding complex were unsuccessful, so we envisaged synthesizing the monomeric palladacycle by a ligand exchange (with chloride) followed by the addition of pyridine. Based on ^{19}F and ^{1}H NMR spectroscopies in solution and the X-ray analysis in the solid state, we identified the product as a mixture of two *cis*/*trans* isomeric complexes with an 85/15% ratio (**Pd**) in favor of the coordination of the palladium at the N^1 and at the C^1 of the fluorinated aryl with the pyridine ligand in the *cis* position with respect to the tetrazine core (Scheme 5 and Fig. 1).

The iridacycle **Ir** and rhodacycle **Rh** were synthesized from the corresponding $[MCl_2Cp^*]_2$ (M = Ir or Rh) precursor, using KOAc as the base in MeOH with 33% and 31% isolated yields, respectively (Scheme 6, top).[11] The X-ray diffraction study of the corresponding metallacycles unambiguously confirmed the coordination mode at N^1 and C^1 (Scheme 6, bottom).

A computational study was then conducted to understand the high selectivity of the metallation. The free energies of palladacycles formed at various nitrogens were computed at the B3LYP/6-311++G(2df,2pd) level. The relative energies for the formed palladacycles Pd(TzInd)(Cl)(pyridine) were 0.0 kcal mol^{-1} for N^1 *cis* and 0.6 kcal mol^{-1} for N^1 *trans*, 9.3 for N^3 *cis* and 12.5 for N^3 *trans*, and more than 24.5 kcal mol^{-1} for the other nitrogen atoms (Fig. 2, see Fig. S-Th1 in the ESI† for all isomers). The metallacycles formed at N^2 are so unstable that the Pd-based fragment prefers to shift to the carbon atom adjacent to N^2, thus lowering its energy by ~1 kcal mol^{-1} (see the ESI, Fig. S-Th1†).

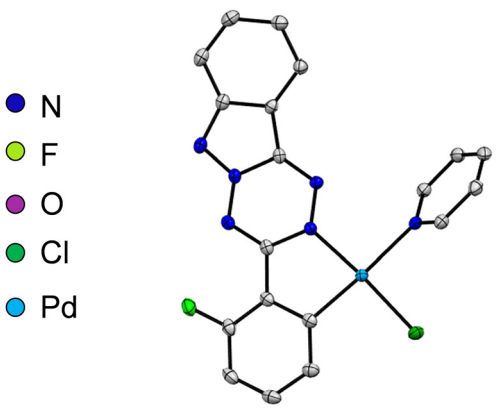

Fig. 1 Molecular structure of **Pd** (thermal ellipsoids at 30% probability, H atoms and one CH_2Cl_2 are omitted for clarity).

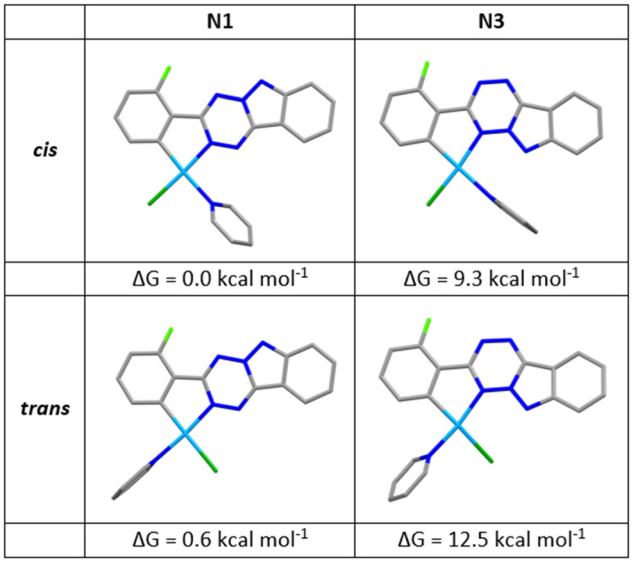

Fig. 2 Metallacycles **Pd** formed at various nitrogens of the tetrazo[1,2-*b*]indazole with the indication of their relative Gibbs free energies (in kcal mol^{-1}). Color scheme: Pd (sky blue), Cl (green), F (light green), N (blue), C (grey).

Applications to transition metal N-directed C–H activation/functionalization

Due to the selective activation of the *ortho*-C–H bond on the N-containing scaffold by transition metals, we evaluated its potential for post-functionalization (Schemes 7 and 8). New C–I and C–OAc were successfully inserted in the *ortho*-position of the aryl of the tetrazo[1,2-*b*]indazole by Pd catalysis in the presence of the appropriate electrophilic source (Scheme 7).[12]

The iodination occurred in the presence of $[Pd(OAc)_2]$ and *N*-iodosuccinimide (NIS) in acetic acid with 66% isolated yield for **23** after 30 minutes under microwave irradiation. Under similar conditions, the more challenging acetoxylation takes place with phenyl iodane diacetate (PIDA) as the electrophilic reagent affording **24** in 51% isolated yield.[8,13]

We then extended our C–H activation toolbox by exploring the use of other transition metals. Based on the abilities of rhodium and iridium in the N-directed oxidative cross-coupling functionalization,[14,15] the direct (hetero)arylation of the 3-

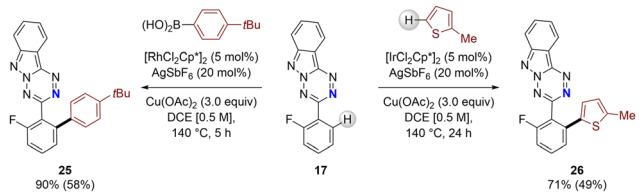

Scheme 8 N-directed oxidative cross-coupling (hetero)arylation of **17**. Conversion based on the consumption of **17** determined by ^{1}H and ^{19}F NMR ($CDCl_3$, 500 MHz and 470 MHz respectively), isolated yields in brackets.

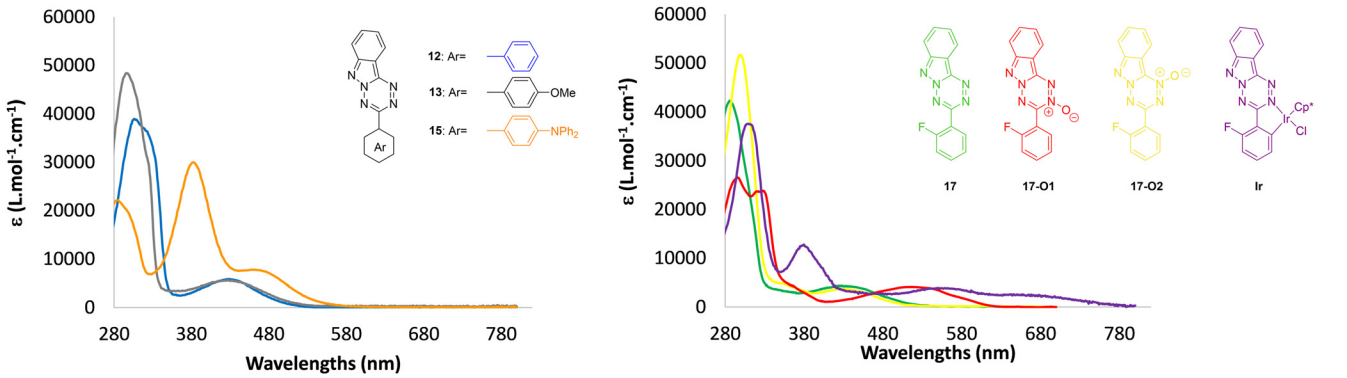

Fig. 3 UV-vis absorption in CH_2Cl_2 of **12** (blue), **13** (grey), **15** (orange) (left); **17** (green), **17-O1** (red), **17-O2** (yellow) and **Ir** (purple) (right).

(2-fluorophenyl)-tetrazo[1,2-*b*]indazole **17** was demonstrated in two oxidative cross-coupling reactions (Scheme 8). These reactions took place with $[Cu(OAc)_2]$ as the oxidant in dichloroethane (DCE) at 140 °C.[16] To couple the 4-*t*-butylphenyl boronic acid, the rhodium catalyst $[RhCl_2Cp^*]_2$ was employed with success to provide **25** in 58% isolated yield. The most challenging dehydrogenative coupling reaction with the 2-methylthiophene was also demonstrated with $[IrCl_2Cp^*]_2$ to form **26** in 49% isolated yield.[17]

Spectroscopic and redox properties of 3-aryltetrazo-[1,2-*b*] indazoles

The spectroscopic properties of **12–22** were investigated in diluted CH_2Cl_2 solutions ($c = 1 \times 10^{-5}$ mol L^{-1}, Fig. 3 and Table S-1 in the ESI†). The electrochemical properties of **12–22** were investigated by cyclic voltammetry in dichloromethane solutions (see the ESI, Fig. S-3 and S-4†).

First, the effect of the (hetero)aryl in the 3-position was investigated (Fig. 3, and Fig. S-3 and S-4 in the ESI†). The tetrazo[1,2-*b*]indazoles **12–22** all display a large absorption with moderate extinction coefficient in the visible range ($\lambda_{max} \sim 435$ nm) assigned to a π–π* transition, regardless of the lateral substituent. Only the presence of the strongly electron donating diphenylamine (DPA) in **15** allows a red-shift of the absorption to 459 nm through the introduction of sufficient charge transfer from the NPh_2 to the electron-deficient TzIn core (see the ESI, Fig. S-Th2†). This is also supported by cyclic voltammetry as **15** is the only compound to display an oxidation wave under these conditions (E_{ox}(**15**) = +1.18 V *vs.* SCE). Such low potential oxidation is characteristic of DPA based derivatives. Please note that all 3-aryl-substituted TzIn display quasi-reversible reduction at low potential in the −0.8 to 0.9 V *vs.* SCE range, as previously observed with such derivatives.[4]

As the effect of the 3-substituent is rather limited, we then investigated the effect of *N*-substitution. While protonation (Fig. S-4†) and oxidation of N^2 has a limited impact on the absorption (λ_{max}(**17-O2**) = 428 nm), the oxidation of N^1 leads to a strong red-shift (λ_{max}(**17-O1**) = 517 nm). This difference is well reproduced by TD-DFT (see the ESI, Fig. S-Th4†). The red-shift is accompanied by an increase of the reduction potential (E_{red}(**17-O1**) = −0.81 V *vs.* SCE, E_{red}(**17-O2**) = −0.89 *vs.* SCE) (see Fig. S-6†).

Finally, the insertion of transition metals *via* the presence of metallacycles also induces a stronger redshift (λ_{max}(Ir) = 675 nm, Fig. 3, and Fig. S-1 and S-2 in the ESI†). These low energy absorptions are characteristic of MLCT transitions in cyclometalated complexes (see also NTO in Fig. S-Th3†).[18]

Note that none of these TzIn show luminescence either in diluted solution or in the solid state.

As a conclusion, the specific chemistry of the N-atom of these novel heteroaromatics is a powerful way to tune their redox properties.

Conclusions

In conclusion, we have reported a two steps protocol for the divergent synthesis of 3-arylated tetrazo[1,2-*b*]indazoles **12–22**, based on a Pd-catalyzed Liebeskind–Srogl cross-coupling reaction followed by our previously reported N-cyclisation process. The N atoms of the TzIn scaffold remain reactive as demonstrated by protonation, selective oxidation (**17-O1** and **17-O2**) and metalations with Pd, Ir and Rh. Additionally, using these transition metals, selective *ortho*-C–H activation/functionalization on the heterocycle was also demonstrated (**23–26**). The effects of all these molecular engineering strategies on the properties of the 3-arylated tetrazoindazoles were studied experimentally and theoretically, revealing that both optical and redox properties can be finely tuned. This study highlights the diversity of the molecular structures and the electronic properties offered by the tetrazo[1,2-*b*]indazole platform and opens up interesting perspectives for its integration into optoelectronic devices.

Experimental section

Procedure for the synthesis of 3-(2-fluorophenyl)-6-aryl-[1,2,4,5]-tetrazine

An oven-dried Schlenk tube equipped with a magnetic stirring bar was sequentially charged with of 3-(methylthio)-6-(2-fluoro-

phenyl)-[1,2,4,5]-tetrazine (1.0 equiv.), [$PdCl_2$(dppf)] (15 mol%), arylboronic acid (2.0 equiv.) and Ag_2O (2.0 equiv.). After 3 cycles of vacuum purging with argon, DMF [0.1 M] solvent was added by syringe. After heating under argon at 60 °C for 20 h, the DMF was removed by rotary evaporation under vacuum. The crude was purified by column chromatography.

Procedure for the synthesis of 3-(aryl)-[1,2,4,5]-tetrazo[1,2-*b*] indazole

As a typical experiment, the 3-aryl-6-(2-fluorophenyl)-[1,2,4,5]-tetrazine (1.0 equiv.) and sodium azide (3.0 equiv.) were introduced in a microwave reaction vessel equipped with a magnetic stirring bar. The DMF [0.125 M] was added, and the reaction mixture was heated at 130 °C under air for 1 h. After cooling down to room temperature, the solvent was removed under vacuum. The crude product was purified by silica gel column chromatography to afford the corresponding product.

Procedure for the direct halogenation/acetoxylation of 3-(2-fluorophenyl)-[1,2,4,5]-tetrazo[1,2-*b*]indazole

As a typical experiment, an oven-dried Schlenk tube equipped with a magnetic stirring bar was charged with 3-(2-fluorophenyl)-[1,2,4,5]-tetrazo-[1,2-*b*]-indazole (1.0 equiv.), NIS or PIDA (2.0 equiv.), [$Pd(OAc)_2$] (10 mol%), and HOAc [0.5 M] under air. The mixture was stirred at 110 °C for 30 min under microwave irradiation (200 Watts). The solvent was removed under vacuum and the crude product was purified by column chromatography on silica using an appropriate ratio of the eluent to afford the desired product.

Procedure for the direct arylation of 3-(2-fluorophenyl)-[1,2,4,5]-tetrazo[1,2-*b*]indazole

As a typical experiment, an oven-dried Schlenk tube equipped with a magnetic stirring bar was charged with 3-(2-fluorophenyl)-[1,2,4,5]-tetrazo-[1,2-*b*]-indazole (1.0 equiv.), 4-*tertio*butylphenyl boronic acid or 2-methylthiophene (3.0 equiv.), [$MCl_2Cp^*]_2$ (5 mol%, M = Rh or Ir), $AgSbF_6$ (20 mol%), Cu$(OAc)_2$ (3.0 equiv.) and dichloroethane [0.5 M] under air. The mixture was stirred at 140 °C for 5 h or 24 h. The solvent was removed under vacuum and the crude product was purified by column chromatography on silica using an appropriate ratio of eluent to afford the desired product.

Procedure for the metallacycle formation by *o*-C–H activation of 3-(2-fluorophenyl)-[1,2,4,5]-tetrazo-[1,2-*b*]-indazole

Palladacycles A-*x* (*x* = 1, 2 and 3). An oven-dried Schlenk tube equipped with a magnetic stirring bar was charged with [$Pd(OAc)_2$] (83 mg, 0.37 mmol, 1 equiv.), **17** (100 mg, 0.37 mmol, 1 equiv.) and HOAc [9.25 mM]. After heating at 80 °C under argon for 16 h, the brown solution was concentrated under vacuum. The crude mixture was dissolved in CH_2Cl_2 and then was filtrated through a pad of Celite (with CH_2Cl_2). The solvent was removed under vacuum and the mixture was recrystallized in a dichloromethane/pentane mixture to afford **Pd_2** as a dark brown powder (120 mg, 75% yield). LiCl (10 mg, 0.23 mmol, 10 equiv.) was added to a solution of **Pd_2** (20 mg, 0.023 mmol, 1 equiv.) in chloroform (5 ml, [4.65 mM]). After 30 min stirring, the solvent was removed under vacuum and then dichloromethane was added [4.65 mM] for better solubility. Pyridine (4 µl, 0.05 mmol, 2 equiv.) was added and the solution was stirred for an additional 30 min giving a bright orange solution. The solution was washed with water then the crude was purified by column chromatography (CH_2Cl_2/MeOH: 90/10). The second fraction was recrystallized in dichloromethane/pentane to afford a mixture of isomers as an orange powder (16 mg, 71% yield).

Iridacycle (Ir) and rhodacycle (Rh). As a typical experiment, an oven-dried Schlenk tube equipped with a magnetic stirring bar was charged with 3-(2-fluorophenyl)-[1,2,4,5]-tetrazo-[1,2-*b*]-indazole ligand **17** (1.0 equiv.), [$MCl_2Cp^*]_2$ (0.5 equiv., M = Ir or Rh) precursor, and KOAc (4.0 equiv.) as the base. After 3 cycles of vacuum purging with argon, MeOH [0.094 M] solvent was added. The mixture was stirred at 60 °C for 14 h, and then filtered through Celite and washed with CH_2Cl_2. The solvent was removed under vacuum and the crude product was purified by column chromatography on silica using an appropriate ratio of eluent to afford the desired metallacycle.

N-oxides (17-O1 and 17-O2)

In a dry Schlenk tube under argon was added H_2O_2 (1.55 ml, 15.1 mmol, 10 equiv.) to trifluoromethanesulfonic anhydride (2.1 ml, 15.1 mmol, 10 equiv.) in dry CH_2Cl_2 (10 ml), and the mixture was stirred for 5 min at 0 °C. Then 3-(2-fluorophenyl)-[1,2,4,5]-tetrazo-[1,2-*b*]-indazole **17** (400 mg, 1.5 mmol, 1 equiv.) was added to the solution at 0 °C and stirred for 5 h. The solvent was removed under vacuum. The product was purified through silica gel column chromatography (CH_2Cl_2/petroleum ether: 40/60) to afford **17-O2** (135 mg, 32%, yellow powder) as the first eluted compound and **17-O1** (148 mg, 35%, red powder) as the second.

Author contributions

Asmae Bousfiha: investigation, methodology, supervision, validation. Oumaima Abidi: investigation, methodology, validation. Louis Lemetayer: investigation, validation. Navya Sood: investigation. Iogann Tolbatov: formal analysis (DFT). Fabien Barrois: formal analysis (DFT). Ahmad Daher: investigation. Hélène Cattey: formal analysis (crystal analysis). Marie Cordier: formal analysis (crystal analysis). Muriel Hissler: funding acquisition, conceptualization, writing – review & editing. Jean-Cyrille Hierso: funding acquisition, conceptualization, writing – review & editing. Paul Fleurat-Lessard: funding acquisition, investigation, conceptualization, supervision, writing – original draft. Pierre-Antoine Bouit: funding acquisition, investigation, conceptualization, supervision, writing – original draft. Julien Roger: funding acquisition, investigation, conceptualization, supervision, writing – original draft.

Conflicts of interest

There are no conflicts to declare.

Acknowledgements

This work was supported by the CNRS, Conseil Régional de Bourgogne (PARI and FEDER programs), by the COMUE UBFC (ISITE UB180013.MUB.IS_SmarTZ; R. J., I. T. and PhD grant for A. D.), by the ANR JCJC program 2018 FITFUN (ANR-18-CE07-0015; R. J. and PhD grant for O. A.) and ANR Pi-Aza (ANR-21-CE07-0024-01, P.-A. B., A. B. and PhD grant for L. L.). Calculations were performed using HPC resources from DSI-CCUB at the Université de Bourgogne. The authors thank the PACSMUB platform for analyses (SATT SAYENS) especially M.-J. Penouilh and Q. Bonnin.

Notes and references

1 (*a*) U. H. F. Bunz, *Acc. Chem. Res.*, 2015, **48**, 1676–1686; (*b*) M. Stępień, E. Gońka, M. Żyła and N. Sprutta, *Chem. Rev.*, 2016, **117**, 3479–3716; (*c*) G. Clavier and P. Audebert, *Chem. Rev.*, 2010, **110**, 3299–3314; (*d*) P. Audebert, E. Kroke, C. Posern and S. H. Lee, *Chem. Rev.*, 2021, **121**, 2515–2544.

2 (*a*) C. L. Anderson, T. Zhang, M. Qi, Z. Chen, C. Yang, S. J. Teat, N. S. Settineri, E. A. Dailing, A. Garzón-Ruiz, A. Navarro, Y. Lv and Y. Liu, *J. Am. Chem. Soc.*, 2023, **145**, 5474–5485; (*b*) G. K. Rastogi, M. L. Deb and P. K. Baruah, *Chem. Commun.*, 2023, **59**, 9642–9645; (*c*) D. Sirbu, J. Diharce, I. Martinic, N. Chopin, S. V. Eliseeva, G. Guillaumet, S. Petoud, P. Bonnet and F. Suzenet, *Chem. Commun.*, 2019, **55**, 7776–7779; (*d*) S. Maier, N. Hippchen, F. Jester, M. Dodds, M. Weber, L. Skarjan, F. Rominger, J. Freudenberg and U. H. F. Bunz, *Angew. Chem., Int. Ed.*, 2023, **62**, e20221403.

3 A. Daher, A. Bousfiha, I. Tolbatov, C. D. Mboyi, H. Cattey, T. Roisnel, P. Fleurat-Lessard, M. Hissler, J.-C. Hierso, P.-A. Bouit and J. Roger, *Angew. Chem., Int. Ed.*, 2023, **62**, e202300571.

4 For other examples of N–N bond formation through azide cyclization, see: (*a*) R. A. Carboni and J. E. Castle, *J. Am. Chem. Soc.*, 1962, **84**, 2453–2454; (*b*) O. Yu. Smirnov, A. M. Churakov, Yu. A. Strelenko and V. A. Tartakovsky, *Russ. Chem. Bull.*, 2008, **57**, 2180–2184; (*c*) A. A. Konnov, M. S. Klenov, A. M. Churakov, Y. A. Strelenko, A. O. Dmitrienko, L. N. Puntus, K. A. Lyssenko and V. A. Tartakovsky, *Asian J. Org. Chem.*, 2018, **7**, 2534–2543; (*d*) S. Gutierrez, A. Arnault, V. Ferreira, A. Artigas, D. Hagebaum-Reignier, Y. Carissan, Y. Coquerel, M.-A. Hiebel and F. Suzenet, *J. Org. Chem.*, 2022, **87**, 13653–13662.

5 C. Testa, E. Gigot, S. Genc, R. Decreau, J. Roger and J.-C. Hierso, *Angew. Chem., Int. Ed.*, 2016, **55**, 5555–5559.

6 Y. Xie, Y. Fang, Z. Huang, A. M. Tallon, C. W. am Ende and J. M. Fox, *Angew. Chem., Int. Ed.*, 2020, **59**, 16967–16973.

7 For other examples of cross-coupling reactions on *s*-tetrazine, see: (*a*) Z. Novak and A. Kotschy, *Org. Lett.*, 2003, **5**, 3495–3497; (*b*) N. Leconte, A. Keromnes-Wuillaume, F. Suzenet and G. Guillaume, *Synlett*, 2007, 204–210; (*c*) L. Pellegatti, E. Vedrenne, J.-M. Leger, C. Jarry and S. Routier, *Tetrahedron*, 2010, **66**, 4683–4389; (*d*) C. Quinton, V. Alain-Rizzo, C. Dumas-Verdes, G. Clavier, L. Vignau and P. Audebert, *New J. Chem.*, 2015, **39**, 9700–9713; (*e*) W. D. Lambert, Y. Fang, S. Mahapatra, Z. Huang, C. W. am Ende and J. M. Fox, *J. Am. Chem. Soc.*, 2019, **141**, 17068–17074; (*f*) E. Ros, A. Prades, D. Forson, J. Smyth, X. Verdaguer, L. Ribas de Pouplana and A. Riera, *Chem. Commun.*, 2020, **56**, 11086–11089; (*g*) Y. Qu, P. Pander, O. Vybornyi, M. Vasylieva, R. Guillot, F. Miomandre, F. B. Dias, P. Skabara, P. Data, G. Clavier and P. Audebert, *J. Org. Chem.*, 2020, **85**, 3407–3416; (*h*) L. V. Hoff, S. D. Schnell, A. Tomio, A. Linden and K. Gademann, *Org. Lett.*, 2021, **23**, 5689–5692.

8 A. Bousfiha, S. Fournier, H. Cattey, P. Fleurat-Lessard, C. H. Devillers, D. Lucas, J.-C. Hierso and J. Roger, *Organometallics*, 2024, **43**, 807–816.

9 (*a*) D. Li, P. Wu, N. Sun, Y.-J. Lu, W.-L. Wong, Z. Fang and K. Zhang, *Curr. Org. Chem.*, 2019, **23**, 616–627; (*b*) H. Wie, H. Gao and J. Shreeve, *Chem. – Eur. J.*, 2014, **20**, 16943–16952.

10 C. D. Mboyi, C. Testa, S. Reeb, S. Genc, H. Cattey, P. Fleurat-Lessard, J. Roger and J.-C. Hierso, *ACS Catal.*, 2017, **7**, 8493–8501.

11 Y.-F. Han and G.-X. Jin, *Chem. Soc. Rev.*, 2014, **43**, 2799–2823.

12 (*a*) S. R. Neufeldt and M. S. Sanford, *Acc. Chem. Res.*, 2012, **45**, 936–946; (*b*) D. A. Petrone, J. Ye and M. Lautens, *Chem. Rev.*, 2016, **116**, 8003–8104.

13 D. Kalyani and M. S. Sanford, *Org. Lett.*, 2005, **7**, 4149–4152.

14 S. Basak, J. P. Biswas and D. Maiti, *Synthesis*, 2021, **53**, 3151–3179.

15 Y. Yang, J. Lan and J. You, *Chem. Rev.*, 2017, **117**, 8787–8863.

16 (*a*) T. Vogler and A. Studer, *Org. Lett.*, 2008, **10**, 129–131; (*b*) X.-L. Lyu, S.-S. Huang, Y.-Q. Huang, Y.-Q. Li, H.-J. Song, Y.-X. Liu and Q.-M. Wang, *J. Org. Chem.*, 2020, **85**, 10271–10282.

17 G. Tan, Q. You and J. You, *ACS Catal.*, 2018, **8**, 8709–8714.

18 Y. Chi and P. T. Chou, *Chem. Soc. Rev.*, 2010, **39**, 638–655.